



Comparative Analysis of Advanced Real-Time Precise Point Positioning Techniques

Mahmoud Abd Rabbou¹, Kamal Ahmed²

Assistant Professor, Department of Civil Engineering, Faculty of Engineering, Cairo University¹²

الملخص العربي

تقليدياً، يمكن لمستخدمي ال GNSS إستعمال تصحيحات MGEX-IGS الدقيقة للمدار و للساعات فقط لتحديد موقع نقطه بدقه PPP في وضع المعالجه البعديه و هو ما يحد من إمكانية إستخدام طريقه تحديد موقع نقطه بدقه PPP في العديد من تطبيقات الملاحة الأنيه. وقد أكدت خدمة الGNSS الدولي (IGS) حديثاً توافر منتجات دقيقه للمدار و الساعات و المتوافره أنيا لأقمار ال GNSS. و لكن تتم معالجة الموديل القياسي الخالي من الايونوسفير لتحديد موقع نقطه بدقه PPP بإستخدام برنامج: (BNC) BKG NTRIP Client للمعالجه الأنيه، و هو ما يحد من دقة تحديد الموقع. في هذا البحث، قمنا بتطوير نموذج رياضي لتحديد مواقع النقط بدقه و مسمي بفارق وحيد بين الاقمار (BSSD) و مرجع التباس متعدد (MAD) للمعالجه الأنيه. يتم في البدايه تنزيل و حفظ ملفات التصحيحات الأنيه و أرساد ال GNSS. ثم يتم تطبيق التصحيحات الأنيه للارصاد المذاعه بإستخدام خوارزميه ببرنامج MATLAB. قمنا بتقييم وقت التقارب و دقه الموقع لموديل ال RT_PPP بإستخدام بيانات تم تجميعها محطات GNSS رباعيه بإجمالي 252 مجموعه قصيره الارصاد. و قد تم تحليل حلول الموقع ذات الساعات الثلاث لتمثل أداء ال RT-PPP في وقت الرصد القصير. بالنسبه للبيانات الخاصه بخمسة أيام، فقد تم تقسيم كل يوم الي ثمانيه جلسات. و تم معالجة كل جلسه علي حدي مما نتج عنه 320 مجموعه من النتائج لإستنتاج تقدير إحصائي لدقة الموقع. و قد تحسنت دقة الموقع ب 30% عند إستخدام موديل ال MAD RT-PPP بدلا من التقنيه القياسيه. ومن جهه أخرى فقد حسن موديل ال BSSD RT-PPP دقة القياس ب 15% بالمقارنه بتقنيه ال RT-PPP القياسيه. كذلك فقد أوضحت النتائج أنه بإستخدام تقنيه ال MAD تم تخفيض وقت التقارب ب 10% بالمقارنه بتقنيه ال RT-PPP القياسيه.

Abstract

Traditionally, GNSS users could use the MGEX-IGS orbit and clock precise corrections only for precise point positioning (PPP) in post processing mode, which confines the accessibility of using PPP to be employed in a wide range of real-time navigation applications. Recently, the International GNSS Service (IGS) has confirmed the availability of open access Real-Time (RT) multi-constellation GNSS precise orbital and clock products. However, the standard ionosphere-free PPP model is processed via the BKG NTRIP Client (BNC) software in real time mode, which limits the positioning accuracy. In this research, we developed a new mathematical PPP model, namely the Between-Satellite-Single-Difference (BSSD) and Multiple-Ambiguity-Datum (MAD), to be processed in real time mode. The real time corrections and GNSS observations files are first downloaded and saved. Real time corrections are applied to the broadcast ephemerides using a MATLAB manuscript. We evaluated the convergence time and positioning accuracy of the RT-PPP model using 320 short data sets collected by GNSS stations that log GPS, GLONASS, Galileo, and BeDou signals. Three-hour position solutions were analyzed to represent the RT-PPP performance in a short observation time. The positioning accuracy was enhanced by 30 % when the MAD RT-PPP technique is applied rather than the standard technique. On the other hand, the BSSD RT-PPP model enhanced the positioning accuracy by 15 % in comparison with the standard RT-PPP technique. In addition, the results show that using MAD technique reduced the convergence time by 10% in comparison with the standard RT-PPP technique.

Key words: GNSS, PPP, Real Time, MGEX-IGS, IGS RTS

1. Introduction

Real-time kinematic (RTK) positioning techniques have been the most dominant techniques for real-time application in both precise positioning and navigation communities for decades. To develop the effectiveness and the efficiency of RTK technique and increase its benefits to RTK users, many private organizations have implemented permanent, Continuously Operating Reference Stations (CORS) networks (Rizos (2002), Rizos et al, 2003 and Snay and Solar, 2008). However, the infrastructure of these networks required an expensive investment to satisfy several factors such as density, quality, functionality, integrity and robustness of the GNSS Network (Choy et al., 2017). The cost and complexity of these concerns represent the main limitations and drawbacks of RTK techniques. Therefore, the precise point positioning (PPP) technique, as proposed by Zumberge (1997), represents one of the best alternative positioning solutions (Kouba and Héroux, 2001, Gao and Chen, 2004). The precise GNSS products provided by the International GNSS Service (IGS) for example, enable the PPP technique to overcome baseline range limitations- However, the significant limitation of the PPP technique is the long convergence required for the ambiguity float solution to converge to ensure centimetre-level positioning accuracy (Collins et al, 2010, Ge et al., 2008, Laurichesse et al,2009, Geng et al., 2010, and Shi and Gao, 2014). Moreover, PPP is confined to post-processing missions due to the delay in the availability of satellite orbital and clock correction product.

Recently, the IGS has confirmed the availability of open access real-time (RT) GNSS precise orbital and clock products. IGS launched the IGS real-time service (IGS RTS) on April 1, 2013 to support its superiority in real-time processing missions (Caissy et al., 2017). The new RT GNSS service is offered to PPP users through a free and easily accessed registration process, which allows for the advantage of obtaining corrections streams. The RT service infrastructure is based on station operators, multiple data centres, and analysis centres around the world. Currently, the RTS streams include both GNSS satellite orbit and satellite clock corrections for broadcast ephemeris, and GNSS observations and broadcast ephemeris streams from globally distributed high-quality GNSS receivers. The multi-GNSS network increased quickly with 170 active stations in October 2016. Fig. 1 shows a map Multi-GNSS capable stations. In addition to the GPS and GLONASS RTS products, several open source tools such as BNC are currently employed with the availability of real-time Galileo orbits graciously provided by German Aerospace Center/ München Technical University DLR/TUM and the Centre National d'Etudes Spatiales CNES real-time analysis centre.

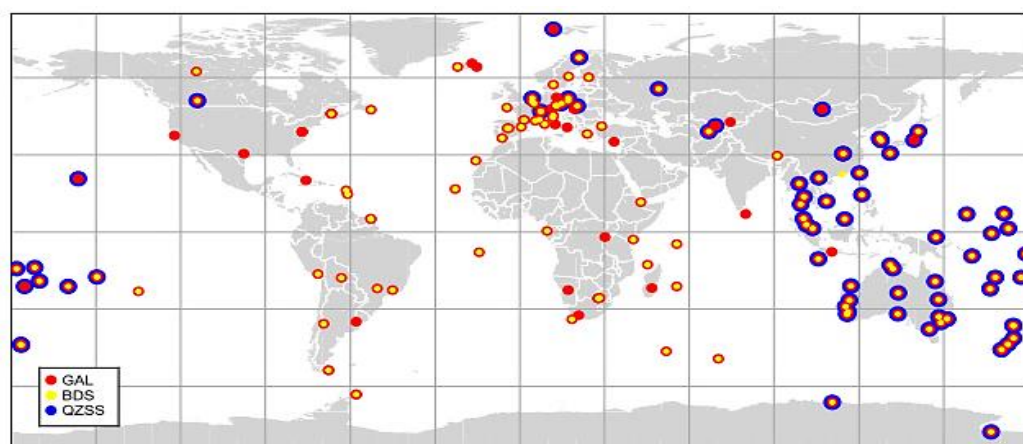


Figure 1: IGS RTS Multi-GNSS Stations (Source: Experiment et al., 2017).

RTS provides SSR Galileo corrections to users. Galileo real-time correction is obtainable as a new product through the CLK93 stream. The main present specifications of CLK93 corrections stream are summarized in Table 1. In addition, CLK93 stream contains Beidou real-time corrections product, which can be attributed to the use of the extrapolated multi-constellation orbits recently obtained from the German Research Center for Geosciences (GFZ), which in turn enabled the CNES real-time analysis centre to provide SSR corrections for Beidou.

Number of research studies discuss the performance of the new real time clock and orbital products. El-Sobeiey and Al-Harbi (2016) evaluate the performance of the real time products on the GPS PPP. Hadas and Bosy (2015) verify the quality of the IGS RTS clock and orbital products over time. Li et al, 2014 assessed the accuracy and reliability of real-time products using multi-GNSS observations namely GPS, GLONASS, Galileo and BeiDou. On other hand, attributing to the availability of real time products, the real time PPP was employed in number of applications. Real-time GPS PPP is used for water vapor estimation and monitoring (Shi et al. (2015), Li et al, (2014), and Lu et al, (2015)). Moreover, Real time PPP is used for resolving ground displacements (e.g. Geng et al, (2016), Mencia et al, (2018)).

In addition, real time PPP can be used in a number of applications, including precise surveying, disaster monitoring, offshore exploration, and others (Geng et al, (2013), Rabbou, M. A. et al, (2015), and Xu et al, (2013)). However, the PPP models employed in such research was the standard ionosphere-free model which limit the performance of the real time PPP. The major drawback of the ionosphere-free PPP model is the long convergence time which represent a major concern for real time navigation applications. This drawback is mainly attribute to the improper modeling of errors and biases, such as the satellite and receiver code biases. The satellite and receiver code bias are lumped to the phase ambiguity parameters which in turn increase the period for ambiguity parameters to be resolved.

Table 1: CLK93 Stream Characteristics (Source: Experiment et al., 2017).

Reference point	APC			
Reference frame	ITRF 2008			
Format	RTCM 3.0			
Satellite constellations	GPS+ GLONASS+ Galileo+ BeiDou			
RTCM Messages	Constellations	Orbits & Clocks	Code biases	Phase biases
	GPS	1060	1059	1265
	GLONASS	1066	1065	1266
	Galileo	1243	1242	1267
	BeiDou	1261	1260	1270
Analysis center	CNES (PPP-WIZARD project)			
Caster IP: Port	http://178.33.109.250:2101			

To enhance the RT PPP, in our research, we used both the between satellite single difference (BSSD) PPP model to cancel out the receiver code biases and the multiple ambiguity datum PPP model to separate the code and phase biases. We evaluated the convergence time and positioning accuracy of the developed RT-PPP models using short data sets collected by multi-GNSS stations. Three-hour position solutions were analyzed to represent the RT-PPP performance in a short observation time.

2. Multi-GNSS RT-PPP Mathematical models

The general ionosphere free linear combination for Multi-GNSS observations can be written as:

$$P_3 = \rho + T^s + c[(dt_r + \beta_r) - (dt^s + \beta^s) + \eta] + \iota \quad (1)$$

$$\Phi_3 = \rho + T^s + c[(dt_r + \beta_r) - (dt^s + \beta^s) + \eta] + [\lambda N - c(\beta_r - \beta^s)] + \varepsilon \quad (2)$$

where P_3 and Φ_3 are the ionosphere free pseudorange and carrier phase observations; ρ is the true geometric range from the antenna phase center of the receiver at reception time to the antenna phase center of the satellite at transmission time; T is the tropospheric delay; c is the speed of light; dt_r is the receiver clock bias; dt^s is the satellite code bias; β_r is the GNSS receiver code bias; η is the GNSS code inter-system bias which is equal zero for GPS observations; ι and ε are relevant system noise and unmodeled residual errors; N is the ionosphere-free ambiguity parameter. One needs to define " λ ".

To completely remove the receiver related bias (β_r) from both the code and phase GNSS observations, between-satellite-single-difference (BSSD) ionosphere-free PPP technique can be used for combined GNSS observations as follows:

$$\Delta P_3 = \Delta \rho + \Delta T^s + c[\Delta(dt^s + \beta^s)] + \Delta \iota \quad (3)$$

$$\Delta \Phi_3 = \Delta \rho + \Delta T^s + c[\Delta(dt^s + \beta^s)] + \Delta[\lambda N + c\beta^s] + \Delta \varepsilon \quad (4)$$

As can be seen the receiver code biases - such as the receiver clock, receiver code bias - are totally removed from both pseudorange and phase observations. However, the satellite code biases still affect the observations. To remove the effect of the receiver and satellite code biases from GNSS phase measurements, multiple ambiguity datum technique (MAD) can be used to separate the code and phase receiver clocks as discussed in Abd Rabbou, et al(2015). Assuming the phase biases are neglected, the mathematical model for MAD PPP technique can be written as follows;

$$\Phi_3^r = \rho + T^s + c[(dt_r + \lambda N^r) - (dt^s) + \mu] + \varepsilon \quad (5)$$

$$\Phi_3 = \rho + T^s + c[(dt_r + \lambda N^r) - (dt^s) + \mu] + [\lambda N - \lambda N^r] + \varepsilon \quad (6)$$

Where Φ_3^r is the reference satellite phase observation (satellite with fixed ambiguity); λN^r is the fixed ambiguity of the reference satellite; μ is the GNSS phase inter-system bias. We can note that the code biases are totally removed from the phase observations.

3. Real-Time Precise Satellite Orbits and Clocks implementation

The RTS products are referenced with respect to the International Terrestrial Reference Frame 2008 (ITRF2008). Orbit corrections are provided as along track, cross track and radial offsets to the broadcast ephemeris in an Earth-centered and Earth-fixed (ECEF)

reference frame. Therefore, the real-time corrections must be transformed from orbital coordinate system to ECEF coordinate system. Three steps are required to compute the real-time satellite position at the current epoch. The orbit corrections $\delta 0$ are defined in the radial ($\delta 0r$), along-track ($\delta 0a$) and cross-track ($\delta 0c$) components. Each component consists of a correction term $\delta 0$ and its velocity $\delta^{\circ}0$. The application algorithm for RTCM-SSR orbit corrections is as follows (Hades and Bosy, 2015):

First, recalculate orbit corrections $\delta 0$ from message reference time to current epoch t:

$$\begin{bmatrix} \delta r \\ \delta a \\ \delta c \end{bmatrix}_{t,orbit} = \begin{bmatrix} \delta r \\ \delta a \\ \delta c \end{bmatrix}_{t_0,orbit} + \begin{bmatrix} \delta^{\circ}r \\ \delta^{\circ}a \\ \delta^{\circ}c \end{bmatrix} (t - t_0) \quad (7)$$

Second, calculate the direction unit vector (e) in radial (e_r), along-track (e_a) and cross-track (e_c) directions to compute the transformation matrix R:

$$e_a = \frac{\dot{r}}{|\dot{r}|} \quad e_c = \frac{r \times \dot{r}}{|r \times \dot{r}|} \quad e_r = e_a \times e_c \quad (8)$$

$$R = [e_r \quad e_a \quad e_c]^T \quad (9)$$

where: r is the satellite broadcast position vector and \dot{r} is satellite broadcast velocity vector.

To transform to ECEF corrections:

$$\begin{bmatrix} \delta x \\ \delta y \\ \delta z \end{bmatrix}_{t,ECEF} = R \begin{bmatrix} \delta r \\ \delta a \\ \delta c \end{bmatrix}_{t,orbit} \quad (10)$$

Third, apply real-time corrections to broadcast coordinates (precise orbit = broadcast orbit – RT corrections):

$$\begin{bmatrix} X \\ Y \\ Z \end{bmatrix}_{t,ECEF} = R \begin{bmatrix} X \\ Y \\ Z \end{bmatrix}_{t,BRD} - \begin{bmatrix} \delta x \\ \delta y \\ \delta z \end{bmatrix}_{t,ECEF} \quad (11)$$

The clock corrections δC are given as offsets to the broadcast ephemeris satellite clock corrections. Similar to the broadcast ephemerides, real-time satellite clock corrections are streamed in the form of polynomial coefficients C_0 ; C_1 , and C_2 . The precise satellite clock correction at any epoch (t) can be calculated by subtracting the real-time correction from the correction computed from the broadcast ephemerides at the same epoch as follows (Hades and Bosy, 2015):

First, recalculate the clock corrections from the message reference time to current epoch (t):

$$\delta C = C_0 + C_1(t - t_0) + C_2(t - t_0)^2 \quad (12)$$

Second, apply the corrections to the broadcast clock

$$t^{sat} = t_{broad}^{sat} - \frac{\delta C}{c} \quad (13)$$

Where: c is the speed of light and t_{broad}^{sat} is the broadcast satellite clock correction

4. Results and analysis

To verify the performance of our RT GNSS PPP models, datasets from eight globally distributed IGS-MGEX stations were processed as shown in Fig. 2. The datasets, used for numerical analysis, were collected at the selected stations on five consecutive days, i.e. January 1–5, 2017. The selected stations were occupied by different types of GNSS receivers as shown in Table 2. Three-hour position solutions were analyzed to represent the RT-PPP performance in a short observation time. For the five-day datasets, each day was divided into eight sessions. Each session was processed separately resulting in a total of 320 sets of results that were then used to derive a statistical estimate for positioning accuracy.

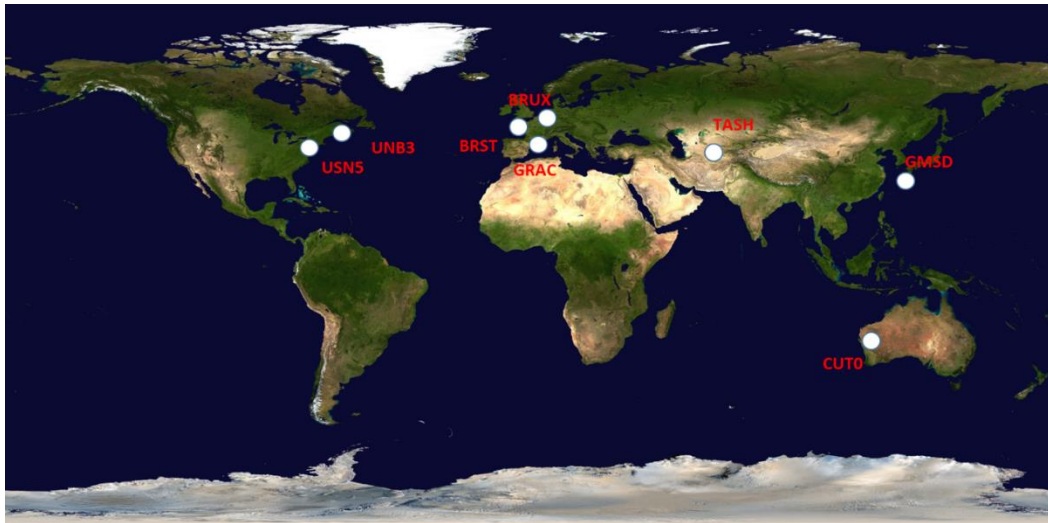


Figure 2. IGS-MGEX stations employed for data collection.

Table 2. MGEX stations selected with different GNSS receivers employed.

<i>Stations selected</i>	<i>GNSS receiver</i>	<i>GNSS data Tracking</i>
<i>BRST, GMSD, CUTO, UNB3 and GRAC</i>	TRIMBLE NETR9	GPS, GLONASS, GALILEO and BeiDou
<i>BRUX</i>	SEPT POLARX4TR	GPS, GLONASS, GALILEO and BeiDou
<i>TASH</i>	JAV_RINGANT_G3T	GPS, GLONASS, GALILEO and BeiDou
<i>USN5</i>	Novatel	GPS, GLONASS and GALILEO

Figure 3 shows the positioning accuracy of station BRUX for the three tested RT-PPP techniques namely, undifferenced, BSSD and MAD ionosphere-free models. The MAD technique provided more accurate positioning with less convergence time than the other techniques. Fig. 3 also shows that the effect of the model is more evident for GPS-only datasets than GNSS datasets. This is due to the additional GNSS observations, which originally improved the positioning accuracy.

Fig. 4 shows the distribution of the 3D positioning errors after 15 minutes for the different RT-PPP GNSS models. The MAD technique provided a more precise solution

for all datasets in comparison with both BSSD and standard undifferenced ionosphere-free models. Table 3 summarizes the statistical analysis for the different RT-PPP GNSS techniques. Statistical analysis suggested that positioning accuracy is enhanced by 30 % when the MAD RT-PPP technique is applied rather than when the standard undifferenced technique was used. The BSSD RT-PPP technique slightly improved the positioning accuracy in comparison with the standard undifferenced RT-PPP technique.

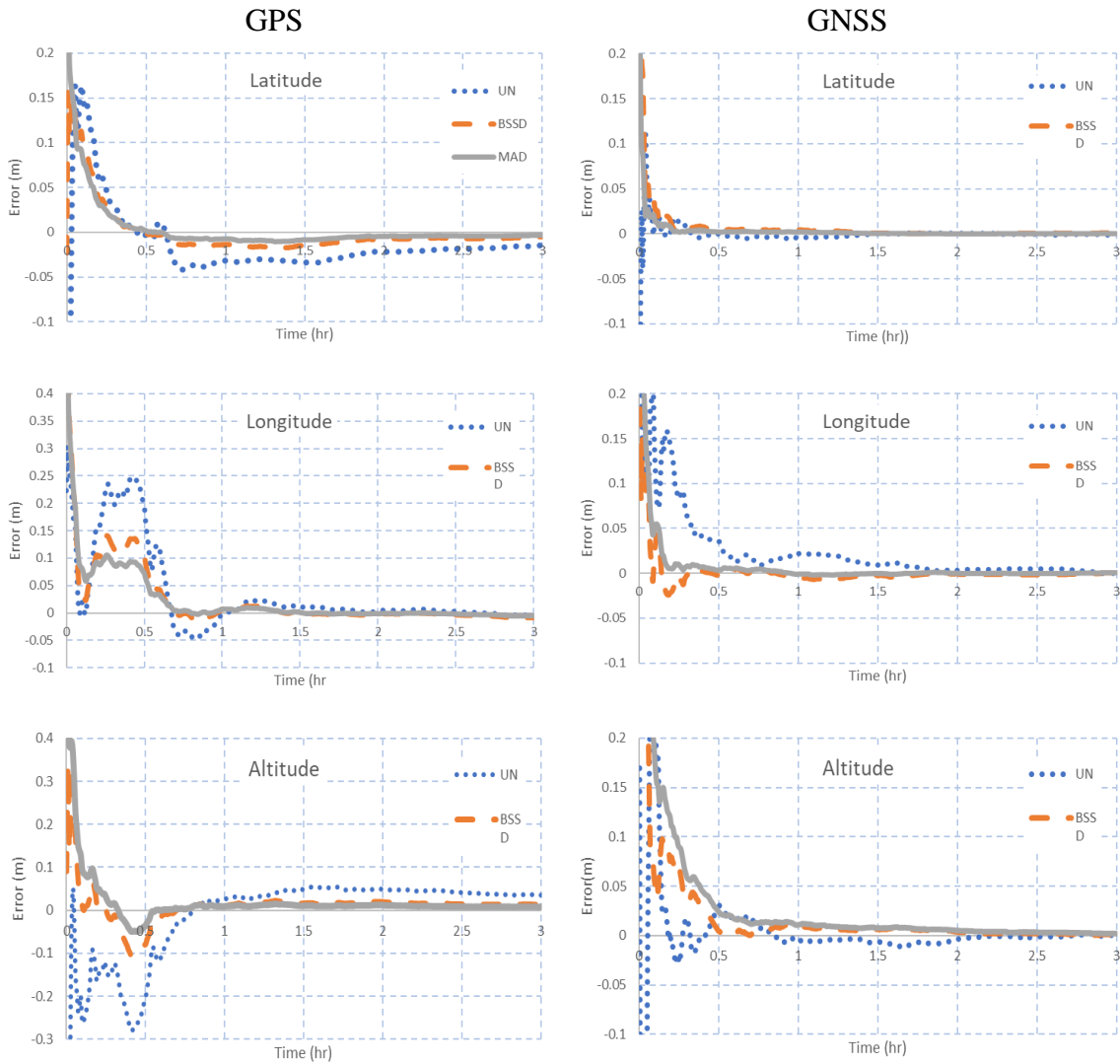


Figure 3. Positioning errors for the Undifferenced, BSSD and MAD RT PPP techniques for station BRUX.

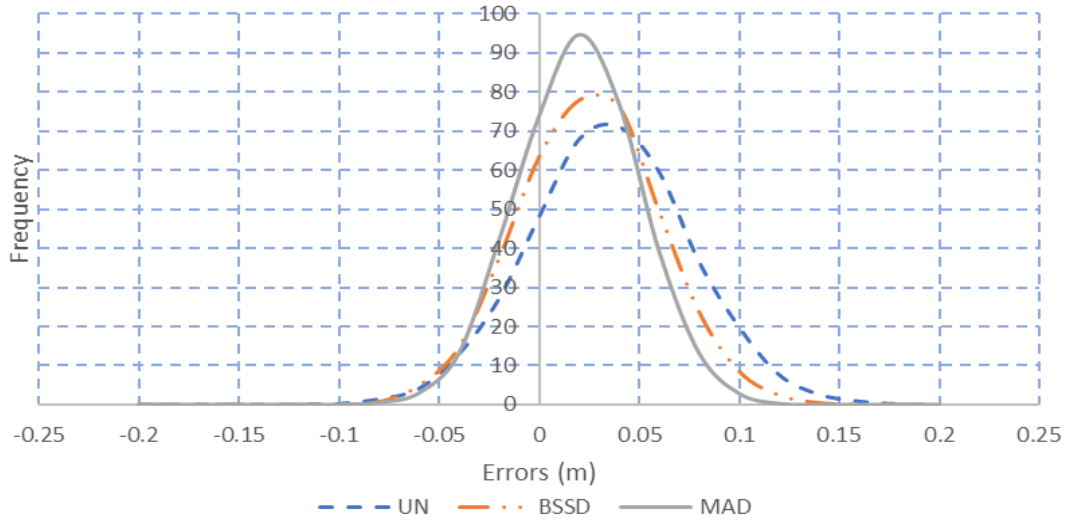


Figure4. Distribution of 3D positioning accuracy after 15 mins for the three RT-PPP techniques.

Table 3. Statistical analysis for the different RT-PPP Models.

RT PPP Models	UN	BSSD	MAD
n	320	320	320
Max (m)	0.21	0.18	0.14
Mean (m)	0.07	0.05	0.04
Min (m)	0.06	0.04	0.39
STD (m)	0.04	0.04	0.03

To evaluate convergence time for the different RT-PPP techniques, Fig. 5 shows the distribution of convergence time for each RT-PPP positioning technique. The MAD technique enhanced convergence time in comparison with the standard undifferenced RT-PPP technique. Table 4 summarizes the statistical analysis for convergence time. The results show that the MAD technique reduces convergence time by 10% in comparison with the standard undifferenced RT-PPP technique. Moreover, maximum convergence time improved by 25 %.

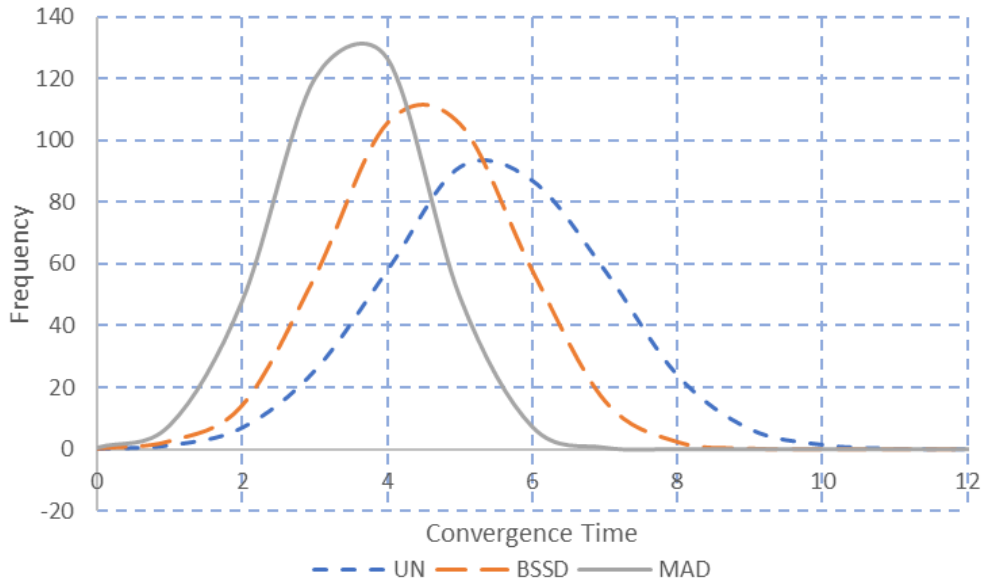


Figure 5. Distribution of convergence time (mins) for the three RT-PPP models.

Table 4. Statistical analysis for the convergence time of different RT-PPP GNSS models.

RT-PPP models	UN	BSSD	MAD
n	320	320	320
max (min)	15	12	11
mean (min)	9	8	7
min (min)	3	4	4
std (min)	1	1	1

5. Conclusions

We developed new real-time multi-GNSS precise point positioning models namely, between satellite single difference (BSSD) and multiple ambiguity datum (MAD) for precise navigation applications. In addition, we assessed the contribution of additional GNSS observations namely GLONASS, Galileo and Beidou on RT PPP positioning accuracy. The RT corrections produced by IGS were saved and applied to the GNSS observations. The results suggested that the positioning accuracy was enhanced by 30 % when the MAD RT-PPP technique was applied rather than the standard undifferenced technique and that the BSSD RT-PPP model was also enhanced. in comparison with the standard undifferenced RT-PPP technique. In addition, the results show that using the MAD technique reduced convergence time by 10% in comparison with the standard undifferenced RT-PPP technique.

6. References

- Caissy, M.; Agrotis, L.; Weber, G.; Hernandez-Pajares, M.; Hugentobler (2017)**, The International GNSS Real-Time Service, 2012. Available online: www.gpsworld.com/gnss-systemaugmentationassistanceinnovation-coming-soon-13044/ (accessed on 12 June 2017).
- Choy, S., Bisnath, S., & Rizos, C. (2017)**, Uncovering common misconceptions in GNSS Precise Point Positioning and its future prospect. *GPS solutions*, 21(1), 13-22.
- Collins, P., Bisnath, S., Lahaye, F., & Héroux, P. (2010)**, Undifferenced GPS ambiguity resolution using the decoupled clock model and ambiguity datum fixing. *Navigation*, 57(2), 123-135.
- Elsobeiey, M., & Al-Harbi, S. (2016)**, Performance of real-time Precise Point Positioning using IGS real-time service. *GPS solutions*, 20(3), 565-571.
- Gao, Y., & Chen, K. (2004)**. Performance analysis of precise point positioning using real-time orbit and clock products. *Positioning*, 1(08), 0.
- Ge, M., Gendt, G., Rothacher, M. A., Shi, C., & Liu, J. (2008)**. Resolution of GPS carrier-phase ambiguities in precise point positioning (PPP) with daily observations. *Journal of Geodesy*, 82(7), 389-399.
- Geng, J., Bock, Y., Melgar, D., Crowell, B. W., & Haase, J. S. (2013)**. A new seismogeodetic approach applied to GPS and accelerometer observations of the 2012 Brawley seismic swarm: Implications for earthquake early warning. *Geochemistry, Geophysics, Geosystems*, 14(7), 2124-2142.
- Geng, J., Teferle, F. N., Meng, X., & Dodson, A. H. (2010)**. Kinematic precise point positioning at remote marine platforms. *GPS solutions*, 14(4), 343-350.
- Geng, T., Xie, X., Fang, R., Su, X., Zhao, Q., Liu, G., & Liu, J. (2016)**. Real-time capture of seismic waves using high-rate multi-GNSS observations: Application to the 2015 Mw 7.8 Nepal earthquake. *Geophysical Research Letters*, 43(1), 161-167.
- Hadas, T., & Bosy, J. (2015)**. IGS RTS precise orbits and clocks verification and quality degradation over time. *GPS solutions*, 19(1), 93-105.
- Kouba, J., & Héroux, P. (2001)**. Precise point positioning using IGS orbit and clock products. *GPS solutions*, 5(2), 12-28.
- Laurichesse, D., Mercier, F., BERTHIAS, J. P., Broca, P., & Cerri, L. (2009)**. Integer ambiguity resolution on undifferenced GPS phase measurements and its application to PPP and satellite precise orbit determination. *Navigation*, 56(2), 135-149.
- Li, X., Dick, G., Ge, M., Heise, S., Wickert, J., & Bender, M. (2014)**. Real-time GPS sensing of atmospheric water vapor: Precise point positioning with orbit, clock, and phase delay corrections. *Geophysical Research Letters*, 41(10), 3615-3621.
- Lu, C., Li, X., Nilsson, T., Ning, T., Heinkelmann, R., Ge, M., ... & Schuh, H. (2015)**. Real-time retrieval of precipitable water vapor from GPS and BeiDou observations. *Journal of Geodesy*, 89(9), 843-856.

Mencin, D., Hodgkinson, K., Mattioli, G., Charles, M., & Sievers, C. (2018, April). Monuments Matter: Resolving Peak Ground Displacements in Real-Time GNSS PPP Solutions as applied to Earthquake Early Warning, an assessment of the M8. 2 September 2017 Tehuantepec Earthquake. In EGU General Assembly Conference Abstracts (Vol. 20, p. 10601).

Rabbou, M. A., & El-Rabbany, A. (2015). Tightly coupled integration of GPS precise point positioning and MEMS-based inertial systems. *GPS solutions*, 19(4), 601-609.

Rizos, C. (2002). Network RTK research and implementation: A geodetic perspective. *Journal of Global Positioning Systems*, 1(2), 144-150.

Rizos, C., Yan, T., Omar, S., Musa, T., & Kinlyside, D. (2003, July). Implementing network-RTK: the SydNET CORS infrastructure. In *The 6th International Symposium on Satellite Navigation Technology Including, Mobile Positioning & Location Services*, Melbourne SatNav.

Shi, J., & Gao, Y. (2014). A comparison of three PPP integer ambiguity resolution methods. *GPS solutions*, 18(4), 519-528.

Shi, J., Xu, C., Guo, J., & Gao, Y. (2015). Real-Time GPS Precise Point Positioning-based precipitable water vapor estimation for rainfall monitoring and forecasting. *IEEE Trans. Geoscience and Remote Sensing*, 53(6), 3452-3459.

Snay, R. A., & Soler, T. (2008). Continuously operating reference station (CORS): history, applications, and future enhancements. *Journal of Surveying Engineering*, 134(4), 95-104.

Xu, P., Shi, C., Fang, R., Liu, J., Niu, X., Zhang, Q., & Yanagidani, T. (2013). High-rate precise point positioning (PPP) to measure seismic wave motions: an experimental comparison of GPS PPP with inertial measurement units. *Journal of geodesy*, 87(4), 361-372.

Zumberge J F, Heflin M B, Jefferson D C, Watkins M M and Webb F H (1997) Precise point positioning for the efficient and robust analysis of GPS data from large networks. *Journal of Geophysical Research*,102(B3): 5005-5018.